Chemical Science

ROYAL SOCIETY OF CHEMISTRY

EDGE ARTICLE

View Article Online
View Journal | View Issue

Cite this: *Chem. Sci.*, 2025, **16**, 21111

All publication charges for this article have been paid for by the Royal Society of Chemistry

Interstellar formation of 1,2-propanediol ($CH_3CH(OH)CH_2OH$) and 1,2-ethenediol (HOCHCHOH)—key precursors to sugars and sugar derivatives

Jia Wang,[ab] Chaojiang Zhang,[ab] André K. Eckhardt *[c] and Ralf I. Kaiser *[ab]

Although sugars and sugar derivatives—molecules critical to the origins of life—have been identified in carbonaceous meteorites with total abundances typically higher than that of amino acids, their underlying formation mechanisms in interstellar environments remain poorly understood. This study reports the first formation of 1,2-propanediol ($CH_3CH(OH)CH_2OH$) and 1,2-ethenediol (HOCHCHOH) in low-temperature model interstellar ices composed of methane (CH_4) and ethylene glycol ($HOCH_2CH_2OH$). 1,2-Propanediol forms *via* the barrierless radical–radical recombination of the methyl ($\dot{C}H_3$) with the 1,2-dihydroxyethyl ($HO\dot{C}HCH_2OH$), while 1,2-ethenediol is produced through the decomposition of ethylene glycol. Utilizing vacuum ultraviolet photoionization reflectron time-of-flight mass spectrometry and isotopic substitution experiments, 1,2-propanediol and its isomer 2-methoxyethanol ($CH_3OCH_2CH_2OH$), along with enols 1,2-ethenediol and vinyl alcohol (CH_2CHOH) were identified in the gas phase during temperature-programmed desorption based on their adiabatic ionization energies and mass-to-charge ratios. Among these compounds, only 1,2-propanediol has not yet been observed in the interstellar medium; these results suggest that it is a promising target for future astronomical detection. Our findings reveal viable abiotic pathways for the formation of biorelevant 1,2-propanediol and 1,2-ethenediol *via* non-equilibrium chemistry in ethylene glycol-containing interstellar ices, advancing our understanding of the fundamental formation mechanisms of sugars and sugar derivatives in deep space.

Received 17th July 2025
Accepted 7th October 2025

DOI: 10.1039/d5sc05315c

rsc.li/chemical-science

Introduction

Since the first identification of methanol (CH_3OH, **1**) in the interstellar medium (ISM) by Ball *et al.* more than half a century ago,[1] alcohols (ROH), where R represents an organic group, have attracted considerable attention from the astronomy,[2–4] astrochemistry,[5–7] astrobiology,[8,9] and physical organic chemistry[10,11] communities mainly due to their central role in the abiotic synthesis of biorelevant molecules essential to the origins of life.[12–14] Within cold molecular clouds, complex organics including alcohols can form *via* non-equilibrium reactions in interstellar ices composed of simple molecules such as water (H_2O), carbon monoxide (CO), carbon dioxide (CO_2), methane (CH_4), and methanol (CH_3OH)[15] driven by ionizing radiation such as ultraviolet (UV) photons and galactic cosmic rays (GCRs).[16] Irradiation of methanol-containing ices with GCR proxies yields glycolaldehyde ($HOCH_2CHO$, **2**),[17] ethylene glycol ($HOCH_2CH_2OH$, **3**),[18] and glycerol ($HOCH_2$-$CH(OH)CH_2OH$, **4**)[19] as key precursors to sugars and phospholipids. Ethylene glycol serves as a molecular building block of the 3-carbon deoxysugar alcohol 1,2-propanediol (propylene glycol, $CH_3CH(OH)CH_2OH$, **5**); the latter represents a critical product in the methylglyoxal pathway in biochemistry by which glucose ($C_6H_{12}O_6$) is metabolized to pyruvate without generating adenosine triphosphate (ATP).[20] Additionally, alcohols can form interstellar enols—alkenes bearing a hydroxyl group connected to a carbon–carbon double bond—such as 1,2-ethenediol (HOCHCHOH, **6**) and vinyl alcohol (CH_2CHOH, **7**),[21,22] which are considered key intermediates in the formation of prebiotic sugars and sugar acids.[21,23–25] Once synthesized, ices bearing these species may become embedded in circumstellar disks during star formation, providing essential ingredients for the formation of comets and planetesimals,[26] which may eventually be delivered to planets like early Earth.[12] Analyses of carbonaceous meteorites such as Murchison and Murray have revealed a variety of sugars and deoxysugar derivatives including **3–5** at high concentrations (*e.g.*, 160 nmol g^{-1} for **4**)[12,27,28] with their total abundance typically exceeding that of

[a]*W. M. Keck Research Laboratory in Astrochemistry, University of Hawaii at Manoa, Honolulu, HI 96822, USA. E-mail: ralfk@hawaii.edu*

[b]*Department of Chemistry, University of Hawaii at Manoa, Honolulu, HI 96822, USA*

[c]*Lehrstuhl für Organische Chemie II, Ruhr-Universität Bochum, Bochum 44801, Germany. E-mail: Andre.Eckhardt@ruhr-uni-bochum.de*

amino acids.[29] However, the fundamental formation mechanisms of these species under astrophysical conditions remain largely conjecture, particularly for the biorelevant 1,2-propanediol (**5**).

In prebiotic chemistry, **5** serves as a fundamental precursor to key biorelevant molecules (Fig. 1). Upon exposure to ionizing radiation, **5** can react with water to form **4**, a molecular building block of sugar alcohols and phospholipids.[13] Oxidation of **5** produces the simplest sugar, glyceraldehyde ($HOCH_2CH(OH)CHO$, **8**), which initiates the synthesis of more complex sugars. Additionally, **5** can be converted into lactaldehyde ($CH_3CH(OH)CHO$, **9**) and methylglyoxal (CH_3COCHO, **10**), the latter of which serves as a direct precursor to pyruvic acid ($CH_3COCOOH$, **11**)—a central metabolic intermediate in the synthesis of amino acids and peptides. Further oxidation of **5** leads to lactic acid ($CH_3CH(OH)COOH$, **12**), which can access the simplest sugar acid, glyceric acid ($HOCH_2CH(OH)COOH$, **13**), thus initiating pathways toward complex sugar acids.[30] Through carbon–carbon or carbon–oxygen bond cleavage, **5** can form **1**, ethanol (CH_3CH_2OH, **14**), *n*-propanol ($CH_3CH_2CH_2OH$, **15**), and i-propanol ($CH_3CH(OH)CH_3$, **16**)—simple alcohols that have been identified in the ISM[1,2,31] and are considered potential precursors to essential biomolecules such as glucose and ribose ($C_5H_{10}O_5$), which are fundamental building blocks of ribonucleic acid (RNA).[9,32] Consequently, **5** represents a fundamental precursor to a suite of sugars and sugar derivatives potentially contributing to the chemical evolution of key biorelevant molecules in extraterrestrial environments. Once formed, these organics may be ultimately delivered to planets like early Earth, as evidenced by their detection in multiple carbonaceous

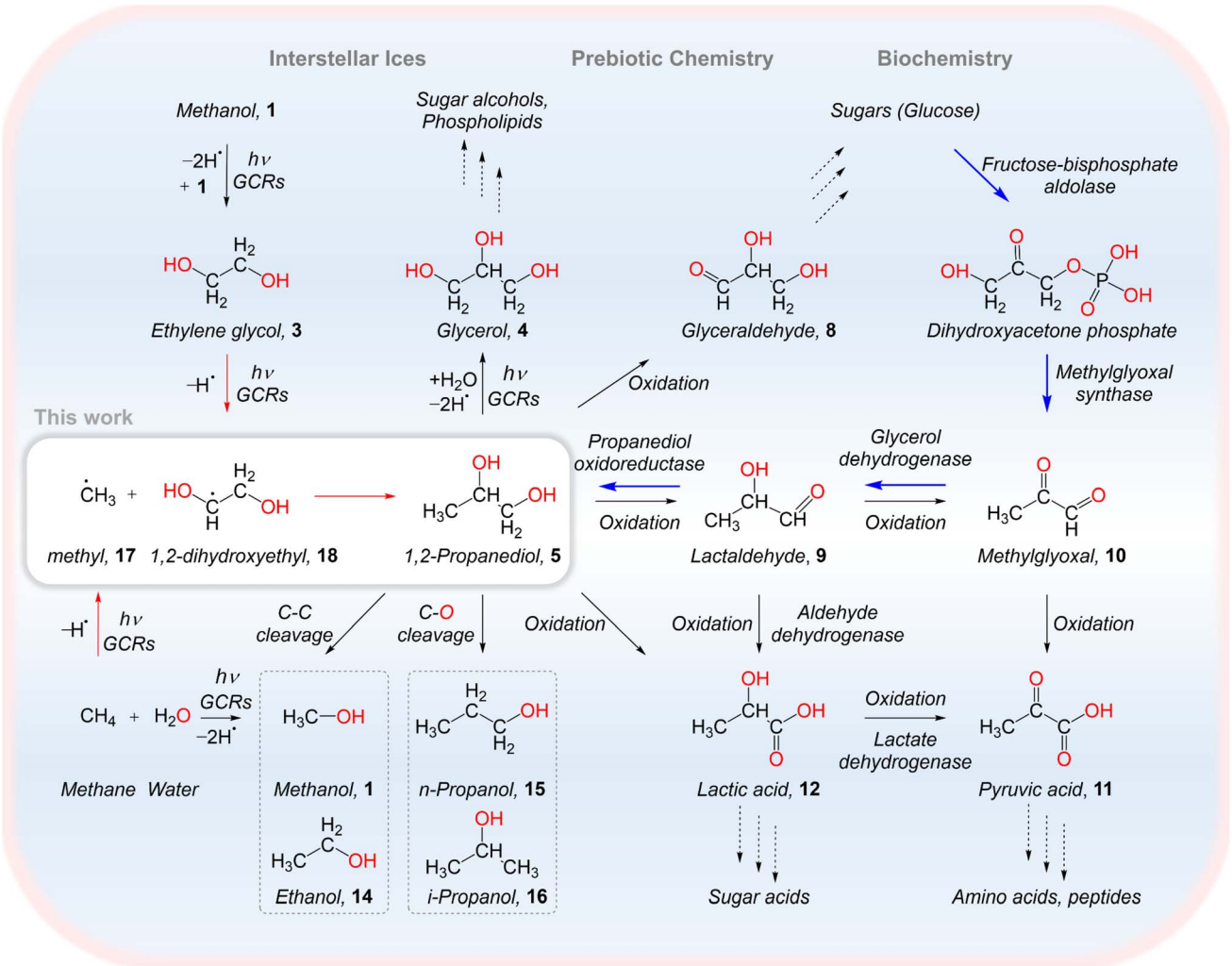

Fig. 1 Proposed formation pathway of 1,2-propanediol in interstellar ices and its potential role as a precursor to biorelevant molecules. 1,2-Propanediol (**5**) is formed *via* radical–radical recombination of the methyl ($\dot{C}H_3$, **17**) radical with the 1,2-dihydroxyethyl ($HO\dot{C}HCH_2OH$, **18**) radical in model interstellar ice carrying methane (CH_4) and ethylene glycol ($HOCH_2CH_2OH$, **3**). Upon radiation by galactic cosmic ray proxies in form of energetic electrons, **5** serves as a molecular building block of sugars and sugar-related molecules such as glycolaldehyde (**8**), lactaldehyde (**9**), and lactic acid (**12**). Additionally, **5** can facilitate the abiotic synthesis of glycerol (**4**), methylglyoxal (**10**), and pyruvic acid (**11**), contributing to the synthesis of essential biorelevant compounds such as phospholipids, amino acids, and peptides. In contemporary biochemistry, **5** is a key product in the methylglyoxal pathway (blue arrows), by which glucose is metabolized to pyruvate without the generation of adenosine triphosphate (ATP).

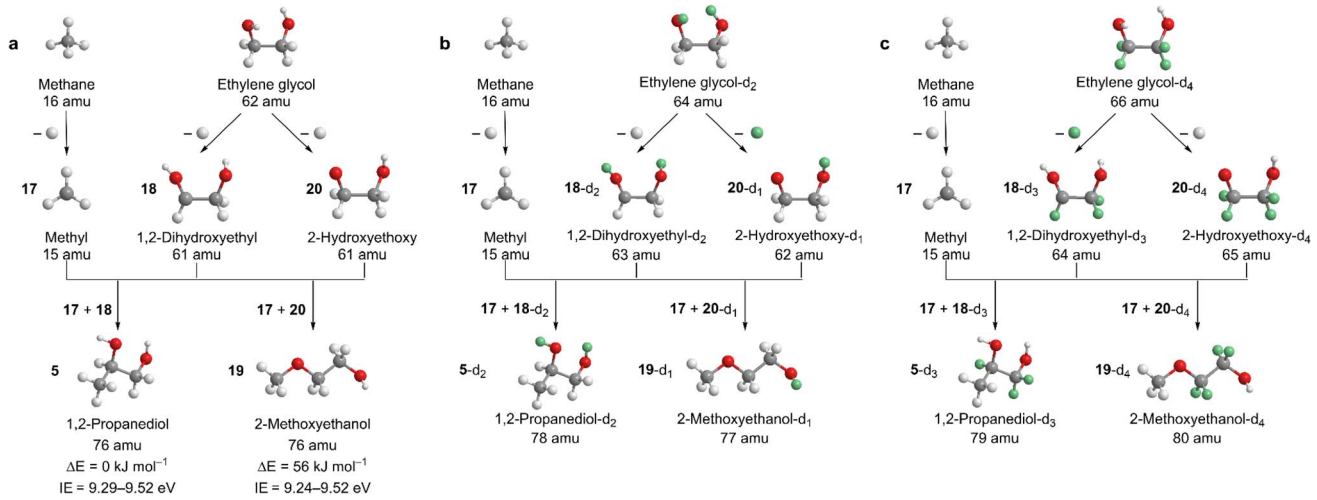

Fig. 2 Reaction schemes leading to 1,2-propanediol and 2-methoxyethanol in irradiated methane–ethylene glycol ices. Barrierless radical–radical recombination of methyl (**17**) with 1,2-dihydroxyethyl (**18**) and 2-hydroxyethoxy (**20**) produce 1,2-propanediol (**5**) and 2-methoxyethanol (**19**), respectively (a–c). The adiabatic ionization energies (IEs) of **5** and **19** are shown as ranges containing all conformers, computed at the CCSD(T)/CBS//B3LYP/cc-pVTZ level of theory. Relative energies (ΔE) are given with respect to the most stable conformer of each structural isomer.[34]

meteorites.[12,27–29] Therefore, elucidating the interstellar formation mechanisms of **5** is crucial to understanding the synthesis pathways of astrobiologically relevant molecules and eventually to the emergence of life.

Here, we present the first preparation of racemic **5** through the barrierless radical–radical recombination of the methyl ($\dot{C}H_3$, **17**) radical with the 1,2-dihydroxyethyl ($HO\dot{C}HCH_2OH$, **18**) radical (Fig. 1 and 2) in interstellar model ices carrying methane and **3**. Low-temperature (5 K) methane–**3** ices were exposed to proxies of GCRs in form of energetic electrons to simulate secondary electrons generated along the tracks of low temperature ices condensed on interstellar nanoparticles (grains) in cold molecular clouds aged up to 2×10^7 years.[33] During the temperature-programmed desorption (TPD) of the irradiated ices, **5** and its isomer 2-methoxyethanol ($CH_3OCH_2CH_2OH$, **19**), along with enols **6** and **7** were identified in the gas phase using vacuum ultraviolet (VUV) photoionization reflectron time-of-flight mass spectrometry (PI-ReToF-MS) in combination with isotopic substitution experiments (SI). These findings reveal viable formation pathways for **5–7** and **19** *via* GCR-driven non-equilibrium chemistries in interstellar ices (Fig. 2), thereby advancing our fundamental understanding of the formation mechanisms of key biorelevant organics—sugars and sugar derivatives—in deep space. Methane–**3** ice can be exploited as a model interstellar ice to comprehensively investigate the formation pathways of **5** and **19**, as both methane and **3** are abundant molecules in the ISM. Methane has been identified in interstellar ices at concentrations of a few percent relative to water.[35,36] Although **3** has only been observed in the gas phase,[37] laboratory simulations have revealed its formation in interstellar ices through surface hydrogenation of carbon monoxide[38] and *via* radical–radical recombination of two hydroxymethyl ($\dot{C}H_2OH$) radicals under exposure to ionizing radiation such as GCRs.[18] Additionally, **3** has been detected in the Murchison meteorite and comets,[4,12] with an abundance of 0.25% with relative to water in comet C/1995 O1 (Hale–Bopp).[4] Therefore, compounds **5–7** and **19** can form in interstellar ices containing methane and **3**. Notably, **6**, **7**, and **19** have been identified in the ISM;[39–41] our results suggest that the hitherto astronomically unobserved **5** is a promising target for future astronomical detection. Once synthesized, these organics may lead to the abiotic formation of key biorelevant compounds (Fig. 1), which can be incorporated into planetesimals and ultimately delivered to planets such as early Earth *via* meteoritic impacts.[12] Such exogenous delivery could have contributed to the emergence of essential biomolecules, providing key insights into the molecular origins of life.

Results

Infrared spectroscopy

Fourier-transform infrared (FTIR) spectroscopy was employed to monitor the chemical evolution of the methane–ethylene glycol ices at 5 K before, during, and after the electron irradiation (Fig. 3 and S1–S3). Detailed assignments of the FTIR spectra are provided in Tables S1–S4. The absorption features of the pristine ices correspond to the fundamental and combination modes of methane and ethylene glycol (**3**).[42–45] After the irradiation, several new absorption features emerged and were deconvoluted into multiple Gaussian functions. In the irradiated CH_4–$HOCH_2CH_2OH$ ice, absorptions at 2976 and 822 cm^{-1} can be attributed to the methyl (CH_3) stretching (ν_{10}) and rocking (ν_{12}) modes of ethane (C_2H_6), respectively (Fig. 3);[46] the methyl stretching (ν_{10}) mode shifts to 2967 cm^{-1} ($^{13}C_2H_6$, ν_{10}) in irradiated $^{13}CH_4$–$HO^{13}CH_2{}^{13}CH_2OH$ ice (Fig. S1). An absorption at 956 cm^{-1} is linked to the CH_2 wagging (ν_7) of ethylene (C_2H_4).[46] The absorptions at 2339 and 2135 cm^{-1} are assigned to the asymmetric stretching (ν_3) of carbon dioxide (CO_2) and the C≡O stretching of carbon monoxide (CO), respectively.[42] These assignments are validated by the detection of $^{13}CO_2$ at

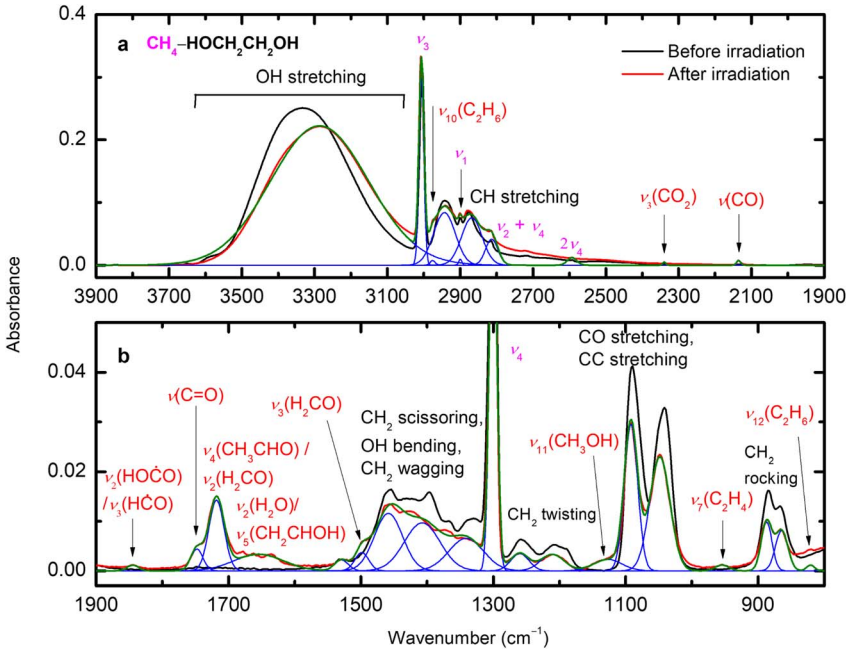

Fig. 3 Infrared spectra of CH_4–$HOCH_2CH_2OH$ ice before (black) and after (red) electron irradiation at 5 K. Deconvolution spectral regions are shown for 3900–1900 cm^{-1} (a) and 1900–800 cm^{-1} (b). The green lines indicate the total fit of the spectra. Detailed assignments are provided in Table S1.

2274 cm^{-1} and ^{13}CO at 2090 cm^{-1} in the irradiated $^{13}CH_4$–$HO^{13}CH_2{}^{13}CH_2OH$ ice.[47] Additional features at 1654, 1499, and 1136 cm^{-1} are linked to water (H_2O, ν_2), formaldehyde (H_2CO, ν_3) and methanol (CH_3OH, ν_{11}), respectively.[42] The band observed at 1718 cm^{-1} is assigned to acetaldehyde (CH_3CHO, ν_4) and/or formaldehyde (ν_2); the formation of both species is confirmed from isotopically labeled ices (Fig. S1–S3).[5,48,49] The absorption at 2070 cm^{-1} in irradiated $^{13}CH_4$–$HO^{13}CH_2{}^{13}CH_2OH$ ice can be attributed to ketene-$^{13}C_2$ ($H_2{}^{13}C^{13}CO$, ν_2).[50] The absorption at 1845 cm^{-1} can be linked to the formyl ($H\dot{C}O$, ν_3) radical and/or *trans*-hydroxycarbonyl ($HO\dot{C}O$, ν_2) radical.[42,51] The formation of *trans*-hydroxycarbonyl is confirmed *via* the detection of $HO^{13}\dot{C}O$ at 1805 cm^{-1} (ν_2) in irradiated $^{13}CH_4$–$HO^{13}CH_2{}^{13}CH_2OH$ ice (Fig. S1).[52] It is worth noting that the absorption at 1654 cm^{-1} observed in the irradiated CH_4–$HOCH_2CH_2OH$ ice can also be connected to the C=C stretching (ν_5) of *syn*-vinyl alcohol (**7**, CH_2CHOH). This assignment is supported by the shift of this band to 1588 cm^{-1} for 7-$^{13}C_2$ ($^{13}CH_2{}^{13}CHOH$), 1575 cm^{-1} for 7-d_3 (CD_2CDOH), and 1641 cm^{-1} for 7-d_1 (CH_2CHOD) in irradiated $^{13}CH_4$–$HO^{13}CH_2{}^{13}CH_2OH$, CH_4–$HOCD_2CD_2OH$, and CH_4–$DOCH_2CH_2OD$ ices, respectively (Fig. S1–S3).[53] However, due to the overlapping absorption features between **3** and the wide suite of irradiation products, FTIR spectroscopy alone is insufficient for a unique identification of complex organics such as **5** and **19**. Therefore, an alternative, more sensitive analytical technique is needed to identify individual reaction products.[54]

Mass spectrometry

Photoionization reflectron time-of-flight mass spectrometry (PI-ReToF-MS) was utilized to identify individual products including $C_3H_8O_2$, $C_2H_4O_2$, and C_2H_4O isomers in the gas phase during TPD based on their desorption temperatures and adiabatic ionization energies (IEs).[54] The PI-ReToF mass spectra of subliming molecules from the irradiated methane–ethylene glycol ices are compiled in Fig. 4.

1,2-Propanediol and 2-methoxyethanol

Focusing on the $C_3H_8O_2$ isomers, a photon energy of 9.60 eV was used to photoionize 1,2-propanediol (**5**, IE = 9.29–9.52 eV) and 2-methoxyethanol (**19**, IE = 9.24–9.52 eV) formed *via* radical–radical recombination of methyl (**17**) with 1,2-dihydroxyethyl (**18**) and 2-hydroxyethoxy (**20**) (Fig. 2). The TPD profile of ion signal at mass-to-charge ratios (m/z) of 76 obtained at 9.60 eV exhibits sublimation events peaking at 182 K (peak I) and 218 K (peak II) for the irradiated CH_4–$HOCH_2CH_2OH$ ice (Fig. 5a). To assign the molecular formula for these sublimation events, a fully ^{13}C-labeled ice mixture ($^{13}CH_4$–$HO^{13}CH_2{}^{13}CH_2$-OH) was used. Replacing CH_4–$HOCH_2CH_2OH$ ice with $^{13}CH_4$–$HO^{13}CH_2{}^{13}CH_2OH$ ice shifts the TPD profile by 3 atomic mass units (amu), from m/z = 76 to m/z = 79 (Fig. 5d), verifying the presence of three carbon atoms. Therefore, the sublimation events observed at m/z = 76 in the irradiated CH_4–$HOCH_2$-CH_2OH ice can be assigned to a molecule of the formula $C_3H_8O_2$. Considering that 9.60 eV photons are capable of ionizing isomers **5** (IE = 9.29–9.52 eV) and **19** (IE = 9.24–9.52 eV), the sublimation events (peaks I and II) of the TPD profile at $m/z = 76$ ($C_3H_8O_2{}^+$) can be attributed to isomer **5** and/or **19**. It is worth noting that ethylene glycol (**3**) exhibits a sublimation event peaking at 214 K (Fig. S4) suggesting that peak II may result from cosublimation with **3**. A blank experiment was conducted without electron irradiation of CH_4–$HOCH_2CH_2OH$

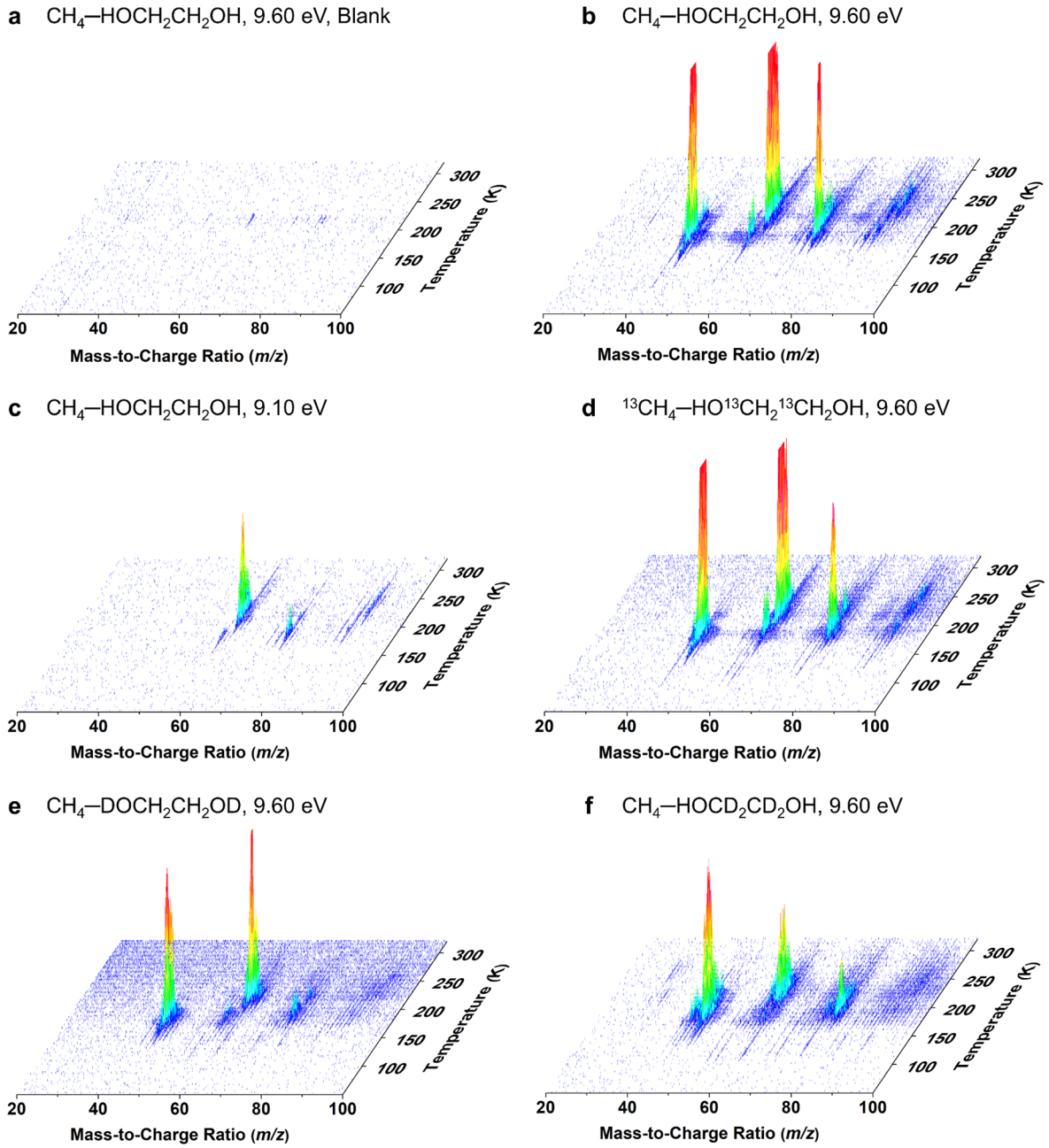

Fig. 4 PI-ReToF-MS data of methane–ethylene glycol ices during TPD. Data were recorded for the unirradiated (blank) CH_4–$HOCH_2CH_2OH$ ice at 9.60 eV (a), the irradiated CH_4–$HOCH_2CH_2OH$ ice at 9.60 eV (b) and 9.10 eV (c), the irradiated $^{13}CH_4$–$HO^{13}CH_2{}^{13}CH_2OH$ ice at 9.60 eV (d), the irradiated CH_4–$DOCH_2CH_2OD$ ice at 9.60 eV (e), and the irradiated CH_4–$HOCD_2CD_2OH$ ice at 9.60 eV (f).

ice under otherwise identical conditions. No ion signal at m/z = 76 was detected except for a tiny and narrow sublimation event between 211 K and 223 K (Fig. 5a), which is likely due to the cosublimation of impurities with **3**. Upon reducing the photon energy to 9.10 eV, at which neither **5** nor **19** can be ionized, peaks I and II are absent, and no sublimation event was detected.

Since the IEs of isomers **5** and **19** overlap, it is imperative to verify their formation through separate experiments at 9.60 eV using isotopically labeled ices including CH_4–$DOCH_2CH_2OD$ ice and CH_4–$HOCD_2CD_2OH$ ice (Fig. 2b and c). From the irradiated CH_4–$DOCH_2CH_2OD$ ice, distinct ion signals at m/z = 78 ($CH_3CH(OD)CH_2OD^+$) for **5** and m/z = 77 ($CH_3OCH_2CH_2OD^+$) for **19** were detected (Fig. 5b). The TPD profiles at m/z = 77 and 78 show two sublimation event (peaks I and II), indicating the that both peaks are linked to **5** and **19**. Similarly, substituting $HOCH_2CH_2OH$ with $HOCD_2CD_2OH$ resulted in the ion signals m/z = 79 ($CH_3CD(OH)CD_2OH^+$) for **5** and m/z = 80 (CH_3OCD_2-CD_2OH^+) for **19**; the TPD profiles of m/z = 79 and 80 show both peaks as well (Fig. 5c), confirming the formation of **5** and **19**. Additional blank experiments without irradiation were conducted at 9.60 eV by adding less than 1% of isomer **5** or **19** into

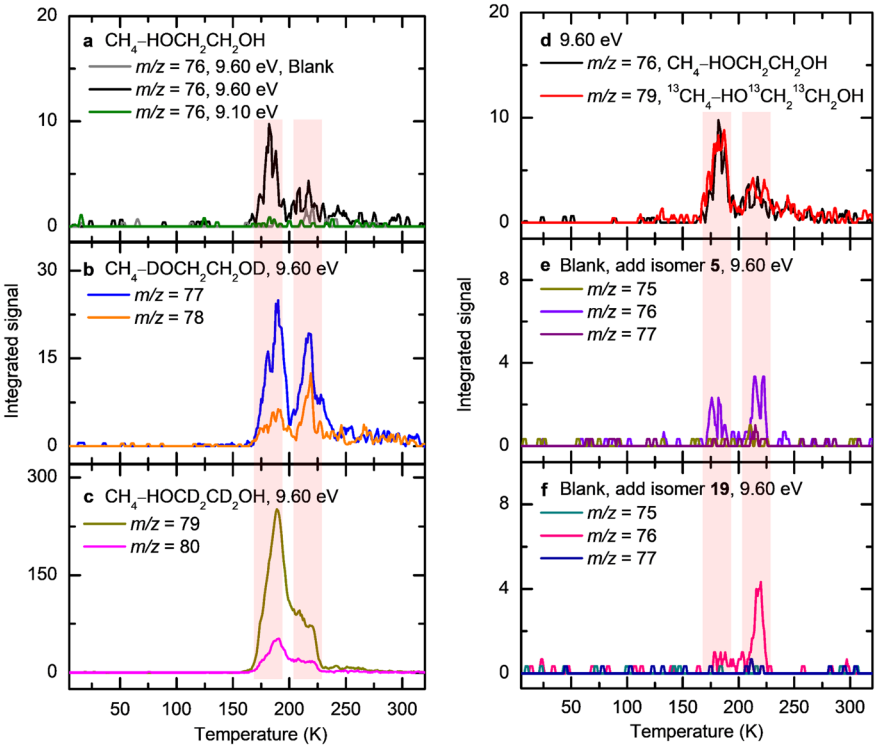

Fig. 5 TPD profiles of $C_3H_8O_2$ isomers from methane–ethylene glycol ices. TPD profiles of $m/z = 76$ from irradiated CH_4–$HOCH_2CH_2OH$ ice measured at 9.60 eV and 9.10 eV (a), $m/z = 77$ and 78 from irradiated CH_4–$DOCH_2CH_2OD$ ice at 9.60 eV (b), $m/z = 79$ and 80 from irradiated CH_4–$HOCD_2CD_2OH$ ice at 9.60 eV (c), and $m/z = 79$ from irradiated $^{13}CH_4$–$HO^{13}CH_2{}^{13}CH_2OH$ ice at 9.60 eV (d). TPD profiles of $m/z = 75$, 76, and 77 in blank experiments adding **5** or **19** were recorded at 9.60 eV (e and f). Red shaded regions indicate the sublimation peaks corresponding to **5** and **19**.

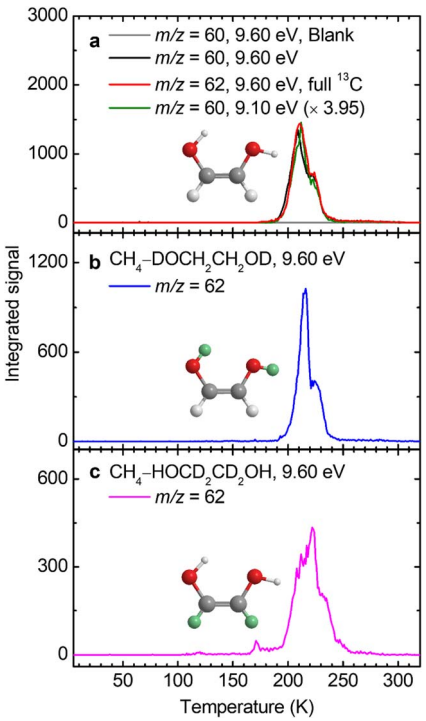

Fig. 6 TPD profiles of $C_2H_4O_2$ isomers from methane–ethylene glycol ices. TPD profiles of $m/z = 60$ from irradiated CH_4–$HOCH_2CH_2OH$ ice measured at 9.60 eV and 9.10 eV (a), $m/z = 62$ from irradiated $^{13}CH_4$–$HO^{13}CH_2{}^{13}CH_2OH$ (a), CH_4–$DOCH_2CH_2OD$ ice (b), and CH_4–$HOCD_2CD_2OH$ ices (c) at 9.60 eV.

the CH_4–$HOCH_2CH_2OH$ ice under otherwise identical conditions. The TPD profile of **5** at $m/z = 76$ revealed two sublimation events centered at 181 K and 220 K (Fig. 5e), while that of **19** exhibited a minor peak centered at 188 K and a major sublimation event peaking at 218 K (Fig. 5f). The latter peak of both isomers likely result from co-sublimation with ethylene glycol. Their first sublimation events agree with peak I (182 K), supporting the assignment of peak I to **5** and **19**.

1,2-Ethenediol

The TPD profile of the ion signal of $m/z = 60$ in irradiated CH_4–$HOCH_2CH_2OH$ ice at 9.60 eV exhibits a sublimation event peaking at 211 K (Fig. 6a). In the irradiated, fully ^{13}C labeled ice ($^{13}CH_4$–$HO^{13}CH_2{}^{13}CH_2OH$), this TPD profile shifts by 2 amu to $m/z = 62$, suggesting the presence of two carbon atoms and confirming a molecular formula of $C_2H_4O_2$. Potential $C_2H_4O_2$ isomers account for this signal can be methyl formate (CH_3OCHO), acetic acid (CH_3COOH), glycolaldehyde ($HOCH_2CHO$), and their enol tautomer, 1,2-ethenediol (**6**). Notably, the sublimation event at $m/z = 60$ remains at a reduced photon energy of 9.10 eV (Fig. 6a). At this energy, only **6** (IE = 8.12–8.43 eV)[55] can be ionized, but methyl formate (IE = 10.59–10.85 eV), acetic acid (IE = 10.43–10.67 eV), and glycolaldehyde (IE = 9.75–10.08 eV) cannot be photoionized.[56] Therefore, the sublimation event at $m/z = 60$ in the irradiated CH_4–$HOCH_2CH_2OH$ ice can be attributed to **6**. The TPD profile of $m/z = 60$ from irradiated

CH_4–$HOCH_2CH_2OH$ ice matches the previously measured TPD profile of **6** obtained from irradiated **1** ice (Fig. S5),[21] confirming the formation of **6**. In irradiated CH_4–$DOCH_2CH_2OD$ ice, the TPD profile of $m/z = 62$ ($DOCHCHOD^+$) agrees with that of $m/z = 60$ ($HOCHCHOH^+$) in irradiated CH_4–$HOCH_2CH_2OH$ ice (Fig. 6b), indicating that **6** forms *via* the dehydrogenation of **3** by losing two hydrogen ($\dot{H}$) atoms—one from the central carbon atom and another from the adjacent carbon atom. This mechanism is consistent with the irradiated CH_4–$HOCD_2CD_2OH$ ice experiment, in which the TPD profile of $m/z = 62$ ($HOCDCDOH^+$) matches that of $m/z = 60$ ($HOCHCHOH^+$) in the irradiated CH_4–$HOCH_2CH_2OH$ ice (Fig. 6c).

Discussion

Having provided compelling evidence for the formation of 1,2-propanediol (**5**), 1,2-ethenediol (**6**), and 2-methoxyethanol (**19**) in irradiated methane–ethylene glycol ices under astrophysical conditions, we now turn to their potential formation mechanisms. First, upon electron irradiation, methane undergoes C–H bond cleavage to produce a methyl ($\dot{C}H_3$) radical and a hydrogen atom ($\dot{H}$) *via* reaction (1) with a reaction endoergicity of 439 kJ mol^{-1}.[57] Recall that ethane (C_2H_6) has been identified by the infrared absorptions of the methyl (CH_3) stretching (ν_{10}) and rocking (ν_{12}) modes, indicating the formation of methyl radicals. The unimolecular decomposition of ethylene glycol (**3**) yield the 1,2-dihydroxyethyl radical (**18**, $HO\dot{C}HCH_2OH$) *via* reaction (2) or the 2-hydroxyethoxy radical (**20**, $\dot{O}CH_2CH_2OH$) *via* reaction (3)[30] with associated endoergicities of 398 and 443 kJ mol^{-1}, respectively.[57,58] The isomerization from **18** to **20** is endoergic by 44 kJ mol^{-1} and proceeds *via* a reaction barrier of 161 kJ mol^{-1} calculated at the AE-CCSD(T)/CBS//AE-MP2/aug-cc-pVTZ level of theory, with negligible H-tunneling contributions at low temperatures.[59] If a methyl radical has a favorable recombination geometry with nearby **18** or **20** radicals, barrierless radical–radical recombination between methyl radical and **18** or **20** can occur, leading to **5** *via* reaction (4) or **19** *via* reaction (5), with reaction energies of −366 and −359 kJ mol^{-1}, respectively.[60,61] X-ray irradiation of matrix-isolated ethanol revealed that 1-hydroxyethyl ($CH_3\dot{C}HOH$) radical is formed preferentially *via* C–H bond cleavage at the central carbon.[62] Recent studies on electron-irradiated CO–CH_3CH_2OH ice indicate the formation of 1-hydroxyethyl and 2-hydroxyethyl ($\dot{C}H_2CH_2OH$) radicals at relatively low irradiation doses.[16] Similarly, the formation of **18** may be more favorable than that of **20**. This is consistent with the isotopically labeled CH_4–$HOCD_2CD_2OH$ experiment, where the ratio of **5**-d_3 to **19**-d_4 was determined as (4.8 ± 0.5): 1 based on their integrated counts. Both **5** and **19** exist numerous conformers (20 for **5** and 12 for **19**), making it difficult to identify which specific conformer(s) formed under our experimental conditions. Accurate quantification of their concentrations or branching ratio would further require their photoionization cross sections at 9.60 eV, which have not yet been experimentally determined.

$$CH_4 \rightarrow \dot{C}H_3 + \dot{H} \quad (1)$$

$$HOCH_2CH_2OH\ (\mathbf{3}) \rightarrow HO\dot{C}HCH_2OH\ (\mathbf{18}) + \dot{H} \quad (2)$$

$$HOCH_2CH_2OH\ (\mathbf{3}) \rightarrow \dot{O}CH_2CH_2OH\ (\mathbf{20}) + \dot{H} \quad (3)$$

$$\dot{C}H_3 + HO\dot{C}HCH_2OH\ (\mathbf{18}) \rightarrow CH_3CH(OH)CH_2OH\ (\mathbf{5}) \quad (4)$$

$$\dot{C}H_3 + \dot{O}CH_2CH_2OH\ (\mathbf{20}) \rightarrow CH_3OCH_2CH_2OH\ (\mathbf{19}) \quad (5)$$

Second, once **18** forms through the decomposition of **3** *via* reaction (2), **6** can be accessed from **18** by the loss of a hydrogen atom (reaction (6)). Recalled that TPD profile of $m/z = 60$ in irradiated CH_4–$HOCH_2CH_2OH$ ice shifts 2 amu to $m/z = 62$ in both irradiated CH_4–$DOCH_2CH_2OD$ and CH_4–$HOCD_2CD_2OH$ ices (Fig. 6b and c), indicating that the formation of **6** involves dehydrogenation of **3** through the loss of one hydrogen atom from the central carbon and another from the adjacent carbon. This reaction is endoergic by 142 kJ mol^{-1}.[57] Similar reaction mechanisms have been demonstrated in recent study on interstellar analog ices, where **7** can form *via* the dehydrogenation of ethanol (**14**) in irradiated carbon monoxide–ethanol ices.[22]

$$HO\dot{C}HCH_2OH\ (\mathbf{18}) \rightarrow HOCHCHOH\ (\mathbf{6}) + \dot{H} \quad (6)$$

Conclusion

This study presents the first abiotic pathways to the biorelevant 1,2-propanediol (**5**) and 1,2-ethenediol (**6**) in low-temperature model interstellar ices composed of methane and ethylene glycol (**3**). These ice mixtures were exposed to energetic electrons as proxies for GCRs, simulating secondary electrons generated along the tracks in interstellar ices in cold molecular clouds aged up to 2×10^7 years.[33] Utilizing VUV photoionization reflectron time-of-flight mass spectrometry and isotopic substitution experiments, **5–6** and 2-methoxyethanol (**19**) were identified in the gas phase during TPD based on their ionization energies and mass-to-charge ratios. These results reveal the formation pathways of **5** and its isomer **19** through radical–radical recombination reactions as well as the enol **6**, providing crucial steps toward a systematic understanding of how sugars and sugar derivatives can be formed in **3**-containing interstellar ices *via* non-equilibrium chemistries. Methane has been detected in interstellar ices at a few percent relative to water,[35,36] and laboratory simulations revealed that **3** can readily form in interstellar analog ices under ionizing radiation such as GCRs.[18] Our results suggest that **5–6** and **19** could be generated in interstellar ices on nanoparticles (interstellar grains) in cold molecular clouds. As dense molecular clouds evolve into star-forming regions, the warmer conditions with rising temperatures (100–300 K) induce the release of complex organics from icy grain mantles into the gas phase.[21,23] Among these, **6** and **19** have been detected toward the G+0.693-0.027 molecular cloud[40] and the massive protocluster NGC 6334I,[41] respectively. Notably, our previous investigation of irradiated low-temperature methanol-bearing ices revealed the formation of **6**,[21] which was subsequently identified toward the G+0.693-0.027 molecular cloud.[40] Given its relatively large dipole moment (2.6 D),[34]

the yet unobserved **5** represents a promising target for future astronomical searches towards star forming regions.

Once synthesized in interstellar ices, **5** can serve as a precursor to critical biorelevant molecules **8–13** (Fig. 1). Additionally, enol **6** can be produced from **2** *via* keto–enol tautomerism and act as a key intermediate in the formose or Butlerov reaction,[63,64] which is fundamental to carbohydrate formation. As a nucleophile, **6** reacts with electrophilic formaldehyde through a favorable six-membered transition state to yield the simplest sugar molecule, **8**.[21] Therefore, **5** and **6** represent essential prebiotic precursors to sugars and sugar derivatives, providing plausible abiotic pathways for their synthesis in extraterrestrial environments. During star formation, icy grains containing these species can be incorporated into circumstellar disks, contributing to the formation of planetesimals and comets. In fact, isomers of $C_2H_4O_2$ and $C_3H_8O_2$ have been detected in dusty coma of comet 67P, with isomers **5** and **19** identified as the most likely contributors to the $C_3H_8O_2$ signal.[3] At least fraction of these complex organics may be delivered to planets like early Earth *via* meteoritic impacts,[12] which has been confirmed by the detection of sugars such as ribose[8] and sugar-related compounds in multiple carbonaceous meteorites.[27–29] Such exogenous delivery presents a plausible prebiotic scenario for the abiotic synthesis of sugars and their derivatives, potentially initiating key chemical processes that led to the emergence of essential biomolecules central to the origins of life.

Finally, it is important to note that the methane–ethylene glycol ices employed in this study serve as simplified model systems to probe the formation mechanisms of $C_2H_4O_2$ and $C_3H_8O_2$ isomers under exposure to GCR proxies. These experiments are designed to investigate fundamental reaction pathways in a controlled environment rather than to replicate the full chemical complexity of interstellar ices. Given that interstellar ices are dominated by water,[15] future studies incorporating water into the ice mixtures may reveal additional reaction pathways and products. For instance, the inclusion of water may facilitate the formation of $C_3H_8O_3$ isomers such as **4** (Fig. 1) in irradiated methane–ethylene glycol–water ices. Additionally, hydroxyl radical formed from water can react with **18** and **20** to produce 1,1,2-ethanetriol ($HOCH_2$-$CH(OH)_2$) and 2-hydroperoxyethanol ($HOCH_2CH_2OOH$), respectively, thereby competing with the pathways leading to **5** and **19**. Future experiments can also investigate the formation of $C_3H_8O_2$ isomers *via* the interaction of GCRs with simple ice mixtures such as CH_4–H_2O and CH_4–CH_3OH. Through radical–radical recombination, additional $C_3H_8O_2$ isomers such as ethoxymethanol ($CH_3CH_2OCH_2OH$), 1-methoxyethanol ($CH_3OCH(OH)CH_3$), dimethoxymethane ($CH_3OCH_2OCH_3$), and ethylmethyl peroxide ($CH_3CH_2OOCH_3$) may form and co-sublime with water or methanol molecules.

Author contributions

R. I. K. designed the experiments; J. W., and C. Z. conducted the experiments; J. W. analyzed the data; A. K. E. carried out the theoretical analysis; J. W., A. K. E. and R. I. K. wrote the manuscript, which was read, revised, and approved by all authors.

Conflicts of interest

The authors declare no conflict of interest.

Data availability

Additional data are available from the corresponding author upon reasonable request.

Essential data are provided in the main text and the supplementary information (SI). Supplementary information: methods (experimental and computational), identification of vinyl alcohol (CH_2CHOH) and its possible formation pathways, FTIR spectra of irradiated methane–ethylene glycol ices (Fig. S1–S3 and Tables S1–S4), TPD profiles of ethylene glycol (Fig. S4) and 1,2-ethenediol (Fig. S5), PI-ReToF-MS data and molecular formula assignments for other ion signals from irradiated methane–ethylene glycol ices (Fig. S6–S12 and Table S5), experimental conditions (Table S6), VUV generation parameters (Table S7), error analysis of IEs (Table S8), and Cartesian coordinates, vibrational frequencies, and IR intensities of computed conformers of 1,2-propanediol and 2-methoxyethanol (Table S9). See DOI: **https://doi.org/10.1039/d5sc05315c**.

Acknowledgements

This work was supported by the U.S. National Science Foundation (NSF), Division of Astronomical Sciences, under grant AST-2403867 awarded to the University of Hawaii at Manoa. The Hawaii group also acknowledges the University of Hawaii at Manoa and the W. M. Keck Foundation for supporting the construction of the experimental setup. The calculations were supported by the Deutsche Forschungsgemeinschaft (DFG, German Research Foundation) under Germany's Excellence Strategy – EXC 2033 – 390677874 – RESOLV.

References

1 J. A. Ball, C. A. Gottlieb, A. E. Lilley and H. E. Radford, *Astrophys. J.*, 1970, **162**, L203.
2 A. Belloche, R. T. Garrod, O. Zingsheim, H. S. P. Müller and K. M. Menten, *Astron. Astrophys.*, 2022, **662**, A110.
3 N. Hänni, K. Altwegg, D. Baklouti, M. Combi, S. A. Fuselier, J. De Keyser, D. R. Müller, M. Rubin and S. F. Wampfler, *Astron. Astrophys.*, 2023, **678**, A22.
4 J. Crovisier, D. Bockelée-Morvan, N. Biver, P. Colom, D. Despois and D. C. Lis, *Astron. Astrophys.*, 2004, **418**, L35–L38.
5 J. Wang, J. H. Marks, A. M. Turner, A. A. Nikolayev, V. Azyazov, A. M. Mebel and R. I. Kaiser, *Phys. Chem. Chem. Phys.*, 2023, **25**, 936–953.
6 G. Fedoseev, K.-J. Chuang, S. Ioppolo, D. Qasim, E. F. van Dishoeck and H. Linnartz, *Astrophys. J.*, 2017, **842**, 52.
7 S. Jheeta, A. Domaracka, S. Ptasinska, B. Sivaraman and N. J. Mason, *Chem. Phys. Lett.*, 2013, **556**, 359–364.

8 Y. Furukawa, Y. Chikaraishi, N. Ohkouchi, N. O. Ogawa, D. P. Glavin, J. P. Dworkin, C. Abe and T. Nakamura, *Proc. Natl. Acad. Sci. U. S. A.*, 2019, **116**, 24440–24445.
9 C. Zhu, A. M. Turner, C. Meinert and R. I. Kaiser, *Astrophys. J.*, 2020, **889**, 134.
10 P. R. Joshi and Y.-P. Lee, *J. Am. Chem. Soc.*, 2024, **146**, 23306–23320.
11 A. K. Eckhardt, M. M. Linden, R. C. Wende, B. Bernhardt and P. R. Schreiner, *Nat. Chem.*, 2018, **10**, 1141–1147.
12 G. Cooper, N. Kimmich, W. Belisle, J. Sarinana, K. Brabham and L. Garrel, *Nature*, 2001, **414**, 879–883.
13 K. Ruiz-Mirazo, C. Briones and A. de la Escosura, *Chem. Rev.*, 2014, **114**, 285–366.
14 T. Mathew, P. M. Esteves and G. K. S. Prakash, *Front. Astron. Space Sci.*, 2022, **9**, 809928.
15 K. I. Öberg, *Chem. Rev.*, 2016, **116**, 9631–9663.
16 J. Wang, C. Zhang, J. H. Marks, M. M. Evseev, O. V. Kuznetsov, I. O. Antonov and R. I. Kaiser, *Nat. Commun.*, 2024, **15**, 10189.
17 S. Maity, R. I. Kaiser and B. M. Jones, *Faraday Discuss.*, 2014, **168**, 485–516.
18 C. Zhu, R. Frigge, A. Bergantini, R. C. Fortenberry and R. I. Kaiser, *Astrophys. J.*, 2019, **881**, 156.
19 R. I. Kaiser, S. Maity and B. M. Jones, *Angew. Chem., Int. Ed.*, 2015, **54**, 195–200.
20 Y.-m. Tao, C.-y. Bu, L.-h. Zou, Y.-l. Hu, Z.-J. Zheng and J. Ouyang, *Biotechnol. Biofuels*, 2021, **14**, 216.
21 N. F. Kleimeier, A. K. Eckhardt and R. I. Kaiser, *J. Am. Chem. Soc.*, 2021, **143**, 14009–14018.
22 J. Wang, C. Zhang, J. H. Marks and R. I. Kaiser, *Astrophys. J.*, 2025, **984**, 138.
23 J. Wang, A. M. Turner, J. H. Marks, C. Zhang, N. F. Kleimeier, A. Bergantini, S. K. Singh, R. C. Fortenberry and R. I. Kaiser, *Astrophys. J.*, 2024, **967**, 79.
24 A. Mardyukov, F. Keul and P. R. Schreiner, *Angew. Chem., Int. Ed.*, 2021, **60**, 15313–15316.
25 J. C. del Valle, P. Redondo, J. Kästner and G. Molpeceres, *Astrophys. J.*, 2024, **974**, 129.
26 R. Visser, E. F. van Dishoeck, S. D. Doty and C. P. Dullemond, *Astron. Astrophys.*, 2009, **495**, 881–897.
27 G. Cooper and A. C. Rios, *Proc. Natl. Acad. Sci. U. S. A.*, 2016, **113**, E3322–E3331.
28 M. Nuevo, G. Cooper and S. A. Sandford, *Nat. Commun.*, 2018, **9**, 5276.
29 S. A. Sandford, M. Nuevo, P. P. Bera and T. J. Lee, *Chem. Rev.*, 2020, **120**, 4616–4659.
30 J. Wang, J. H. Marks, R. C. Fortenberry and R. I. Kaiser, *Sci. Adv.*, 2024, **10**, eadl3236.
31 B. Zuckerman, B. Turner, D. Johnson, F. Clark, F. Lovas, N. Fourikis, P. Palmer, M. Morris, A. Lilley and J. Ball, *Astrophys. J.*, 1975, **196**, L99–L102.
32 C. Zhang, V. Leyva, J. Wang, A. M. Turner, M. Mcanally, A. Herath, C. Meinert, L. A. Young and R. I. Kaiser, *Proc. Natl. Acad. Sci. U. S. A.*, 2024, **121**, e2320215121.
33 A. G. Yeghikyan, *Astrophysics*, 2011, **54**, 87–99.
34 L. Noriega, L. A. González-Ortiz, F. Ortíz-Chi, A. Quintal, S. I. Ramírez and G. Merino, *J. Phys. Chem. A*, 2024, **128**, 9964–9971.
35 J. H. Lacy, J. S. Carr, N. J. Evans II, F. Baas, J. M. Achtermann and J. F. Arens, *Astrophys. J.*, 1991, **376**, 556.
36 M. K. McClure, W. R. M. Rocha, K. M. Pontoppidan, N. Crouzet, L. E. U. Chu, E. Dartois, T. Lamberts, J. A. Noble, Y. J. Pendleton, G. Perotti, D. Qasim, M. G. Rachid, Z. L. Smith, F. Sun, T. L. Beck, A. C. A. Boogert, W. A. Brown, P. Caselli, S. B. Charnley, H. M. Cuppen, H. Dickinson, M. N. Drozdovskaya, E. Egami, J. Erkal, H. Fraser, R. T. Garrod, D. Harsono, S. Ioppolo, I. Jiménez-Serra, M. Jin, J. K. Jørgensen, L. E. Kristensen, D. C. Lis, M. R. S. McCoustra, B. A. McGuire, G. J. Melnick, K. I. Öberg, M. E. Palumbo, T. Shimonishi, J. A. Sturm, E. F. van Dishoeck and H. Linnartz, *Nat. Astron.*, 2023, **7**, 431–443.
37 J. M. Hollis, F. J. Lovas, P. R. Jewell and L. H. Coudert, *Astrophys. J.*, 2002, **571**, L59–L62.
38 G. Fedoseev, H. M. Cuppen, S. Ioppolo, T. Lamberts and H. Linnartz, *Mon. Not. R. Astron. Soc.*, 2015, **448**, 1288–1297.
39 B. E. Turner and A. J. Apponi, *Astrophys. J.*, 2001, **561**, L207–L210.
40 V. M. Rivilla, L. Colzi, I. Jiménez-Serra, J. Martín-Pintado, A. Megías, M. Melosso, L. Bizzocchi, Á. López-Gallifa, A. Martínez-Henares, S. Massalkhi, B. Tercero, P. de Vicente, J.-C. Guillemin, J. García de la Concepción, F. Rico-Villas, S. Zeng, S. Martín, M. A. Requena-Torres, F. Tonolo, S. Alessandrini, L. Dore, V. Barone and C. Puzzarini, *Astrophys. J., Lett.*, 2022, **929**, L11.
41 Z. T. P. Fried, S. J. El-Abd, B. M. Hays, G. Wenzel, A. N. Byrne, L. Margulès, R. A. Motiyenko, S. T. Shipman, M. P. Horne, J. K. Jørgensen, C. L. Brogan, T. R. Hunter, A. J. Remijan, A. Lipnicky, R. A. Loomis and B. A. McGuire, *Astrophys. J., Lett.*, 2024, **965**, L23.
42 M. Bouilloud, N. Fray, Y. Benilan, H. Cottin, M. C. Gazeau and A. Jolly, *Mon. Not. R. Astron. Soc.*, 2015, **451**, 2145–2160.
43 C. J. Bennett, C. S. Jamieson, Y. Osamura and R. I. Kaiser, *Astrophys. J.*, 2006, **653**, 792–811.
44 P. Buckley and P. A. Giguère, *Can. J. Chem.*, 1967, **45**, 397–407.
45 R. L. Hudson, M. H. Moore and A. M. Cook, *Adv. Space Res.*, 2005, **36**, 184–189.
46 M. J. Abplanalp and R. I. Kaiser, *Phys. Chem. Chem. Phys.*, 2019, **21**, 16949–16980.
47 S. Maity, R. I. Kaiser and B. M. Jones, *Phys. Chem. Chem. Phys.*, 2015, **17**, 3081–3114.
48 M. M. Wohar and P. W. Jagodzinski, *J. Mol. Spectrosc.*, 1991, **148**, 13–19.
49 T. Butscher, F. Duvernay, G. Danger and T. Chiavassa, *Astron. Astrophys.*, 2016, **593**, A60.
50 R. L. Hudson and M. J. Loeffler, *Astrophys. J.*, 2013, **773**, 109.
51 D. E. Milligan and M. E. Jacox, *J. Chem. Phys.*, 2004, **41**, 3032–3036.
52 M. E. Jacox, *J. Chem. Phys.*, 1988, **88**, 4598–4607.
53 M. Rodler, C. E. Blom and A. Bauder, *J. Am. Chem. Soc.*, 1984, **106**, 4029–4035.

54 A. M. Turner and R. I. Kaiser, *Acc. Chem. Res.*, 2020, **53**, 2791–2805.
55 G. Y. Matti, O. I. Osman, J. E. Upham, R. J. Suffolk and H. W. Kroto, *J. Electron Spectrosc. Relat. Phenom.*, 1989, **49**, 195–201.
56 N. F. Kleimeier and R. I. Kaiser, *J. Phys. Chem. Lett.*, 2022, **13**, 229–235.
57 B. Ruscic and H. Bross, *Active Thermochemical Tables (ATcT) values based on ver. 1.202 of the Thermochemical Network*, 2021, **https://ATcT.anl.gov**.
58 C. F. Goldsmith, G. R. Magoon and W. H. Green, *J. Phys. Chem. A*, 2012, **116**, 9033–9057.
59 T. Wang and J. H. Bowie, *Org. Biomol. Chem.*, 2012, **10**, 3219–3228.
60 J. P. Guthrie, *Can. J. Chem.*, 1977, **55**, 3562–3574.
61 M. Vasiliu, K. Guynn and D. A. Dixon, *J. Phys. Chem. C*, 2011, **115**, 15686–15702.
62 P. V. Zasimov, E. V. Sanochkina, D. A. Tyurin and V. I. Feldman, *Phys. Chem. Chem. Phys.*, 2023, **25**, 4624–4634.
63 R. Breslow, *Tetrahedron Lett.*, 1959, **1**, 22–26.
64 C. Appayee and R. Breslow, *J. Am. Chem. Soc.*, 2014, **136**, 3720–3723.